International Journal of Gerontology 6 (2012) 20–26

Contents lists available at SciVerse ScienceDirect

International Journal of Gerontology

journal homepage: www.ijge-online.com

Original Article

New Application of Bioelectrical Impedance Analysis by the Back Propagation Artificial Neural Network Mathematically Predictive Model of Tissue Composition in the Lower Limbs of Elderly People☆,☆☆

Tsang-Pai Liu [1,2], Ming-Feng Kao [3], Tsong-Rong Jang [4], Chia-Wei Wang [3], Chih-Lin Chuang [5], Jay Chen [6], Yu-Yawn Chen [3]*, Kuen-Chang Hsieh [7]**

[1] *Department of Surgery, Mackay Memorial Hospital, Taipei, Taiwan,* [2] *Mackay Medicine, Nursing, and Management College, Taipei, Taiwan,* [3] *Department of Physical Education, National Taiwan College of Physical Education, Taichung, Taiwan,* [4] *Athletics Department and Graduate School, National Taiwan College of Physical Education, Taichung, Taiwan,* [5] *Jen–Ai Hospital, Taichung, Taiwan,* [6] *Department of Laboratory Medicine, Hualian Armed Forces General Hospital, Hualian, Taiwan,* [7] *Research Center, Charder Electronic Co., Ltd., Taichung, Taiwan*

ARTICLE INFO

Article history:
Received 17 September 2010
Received in revised form
11 November 2010
Accepted 25 November 2010
Available online 23 March 2012

Keywords:
back propagation artificial neural network (BP–ANN),
bioelectrical impedance analysis (BIA),
dual–energy X–ray absorptiometry,
elderly,
fat–free mass (FFM)

SUMMARY

Background: The accurate evaluation of muscle mass by a non–invasive and easy method is the first step to help prevent falling events in elderly people.
Methods: To develop greater predictive accuracy and precision in the measurement of body composition in lower limbs by bioelectrical impedance analysis (BIA), the Back Propagation Artificial Neural Network (BP–ANN) was used to calculate predictive results and was compared with data from dual–energy X–ray absorptiometry (DXA) in 22 male and 16 female elderly people in Taiwan. Fat–free mass (FFM), tissue weight, and fat mass (FM) of the lower limbs were directly measured by DXA, and the BIA values (Z) of left side hand to right side foot in the standing position were measured by BIA. The parameters of height, weight, age, gender and BIA values were combined to create the BP–ANN mathematical model, which was developed to predict the FFM and FM in lower limbs in elderly.
Result: A relatively lower correlation coefficient (r^2) of 0.964 and standard deviation (2SD) of 0.01 ± 3.64% were obtained for the prediction of FFM and FM by BIA with the BP–ANN mathematical model, whereas the linear regression analyzing model had an r^2 value of 0.845 and 2SD of 0.12 ± 7.68%, respectively. The performance of the BP–ANN mathematical model at BIA measurement was superior to that of the current linear regression model.
Conclusion: In summary, the greater predictive accuracy and precision made the application of BIA with the BP–ANN mathematical model more feasible for the clinical measurement of FM and FFM in the lower limbs of elderly people.

1. Introduction

It is well known that falling accidents often occur due to frailty in the elderly. Sarcopenia in elderly is associated with functional impairment during the aging process[1]. Sarcopenia was also defined as a height–adjusted appendicular muscle mass in older adults of less than two or more SD from that of the normal population[2,3]. Monitoring of the occurrence of sarcopenia in the elderly is important to reduce the incidence of falling and frailty in the elderly.

Due to great effects of nutritional status on morbidity, mortality, and prognosis, precise measurement of body composition in these people should be regularly done in the clinic. Fat–free mass (FFM) decreases with age in the elderly[4,5], and the fat mass (FM) augments with age[5–7]. In particular, this increase of FM and decrease of FFM in the lower limbs, which results in loss of muscle strength[8], is a major contributing factor to falling accidents in the elderly[9]. Precise measurement of body composition in elderly people is important in regular clinical tests[10]. Present measurements, such as dual–energy X–ray absorptiometry (DXA), computed

☆ This study was supported in part by the Charder Electronic Co., LTD.
☆☆ All contributing authors declare no conflict of interest.
* Correspondence to: Yu-Yawn Chen, Department and Graduate School of Physical Education, National Taiwan College of Physical Education, Taichung, Taiwan.
** Co-correspondence to: Kuen-Chang Hsieh, Research Center, Charder Electronic Co., Ltd, No. 103, Guozhong Rd., Dali City, Taichung County 41262, Taiwan.
E-mail addresses: yu11.tw@yahoo.com.tw (Y.-Y. Chen), abaqus0927@yahoo.com.tw (K.-C. Hsieh).

1873-9598/$ – see front matter
doi:10.1016/j.ijge.2011.09.025

tomography (CT), magnetic resonance imaging, air−displacement plethysmography, underwater weighing, neutron activation analysis and dilution methods have many limitations when used for this application[11]. For elderly people with a disability, non−invasive, simple, safe, quick and non−expensive measurement of body composition by bioelectrical impedance analysis (BIA) is appropriate and feasible during regularly clinical tests[12,13].

Measurement of whole body FFM, FM and total body weight (TBW) by measuring whole body BIA has been well studied and applied; however, measurement of body compositions in every single segmental BIA are needed more and more to meet the requirements of clinical application[14–19]. Eight−polar BIA has been used in multiple segmental body compositions when people are in the standing position for assessment of athletes and in weight control[20–22]; but use of this method has been limited to some special cohorts rather than in elderly people[23,24].

The present application of BIA for the estimation of body composition is based on the use of 2−C, 3−C or 4−C models combined with other parameters such as height, weight, age, gender, and race within some specific cohorts to create linearly predictive equations by linear regression analysis. The linearly predictive equations that were created with these parameters aimed to describe the relationship between independent variables and dependent variables[25]. Application of linear regression analysis on single independent variables and single dependant variables is suitable; however, multiple parameters, especially when interactions exist between the parameters, will result in errors in the predictive equation. Besides the most popular method for outcome prediction, artificial neural networks (ANNs)[26–33], there are other mathematical methods such as logistic regression[34], disscriminant analysis and recursive partitioning[35]. The ANN model has performed well, with greater precision and accuracy in the prediction of intercellular fluid and TBW in patients with chronic hemodialysis than that of the linear regression model[36]. Rarely, ANN models have been used to predict body compositions such as FFM, FM and each segmental tissue's weight. Whether greater precision and accuracy can be obtained by prediction of each segmental tissue's weight and other body compositions in elderly patients in a standing position by use of BIA with ANN mathematical model is an interesting issue.

The present study will focus on the development of the novel mathematical model of Back Propagation Artificial Neural Network (BP−ANN) in BIA measurement. This is a modified BIA instrument with automatically changeable models in the standing position, designed to accurately predict the body compositions in the lower limbs in elderly patients. Simultaneously, these parameters were also measured by high resolution and low radiation DXA[37,38]. The precision and accuracy of prediction of body composition by BIA measurements with the BP−AAN mathematical model was compared with that of the linear regression model.

2. Methods

2.1. Subjects

22 male and 16 female elderly patients, who were over 55 years old and from the Taichung district of Taiwan, provided informed formal consent in writing. These healthy elderly people, who had no chronic diseases such as diabetes mellitus, cancer, nephrotic syndrome, hypertension, hepatitis−related diseases, chronic pulmonary diseases, or artificial hearts with assist devices or any artificial electrical implantation, were enrolled. Permission for the study was given by the Institutional Review Board (IRB) of the Advisory Committee at Jen−Ai Hospital in Taiwan. Participants were not allowed to consume any alcoholic beverages within 48 h and were not allowed administration of any diuretic drugs within 7 days before the experimental period. Participants were also not allowed to urinate for the 30 minutes before and during the experiment. Baseline data are shown in Table 1.

Table 1
Characteristics of the participants in the present study.

	Male (n = 22)		Female (n = 16)	
	Mean (SD)	Range	Mean (SD)	Range
Age (years)	61.15 (5.15)	55.4−71.0	60.25 (4.90)	55.1−69.2
Height (cm)	165.5 (6.3)	155.0−180.2	153.5 (6.1)	142.1−165.2
Weight (kg)	69.95 (6.98)	57.0−85.3	62.12 (8.84)	45.5−82.1
BMI (kg/m^2)	25.18 (3.95)	19.92−35.28	26.42 (3.95)	20.94−36.49

BMI, body mass index.

Standard electrodes for calibration of electricity impedance at 500 ohm were used to calibrate the instrument before and after modification, according to the standard calibrating protocol offered by Bodystat, Ltd. The data measured before and after modification were analyzed by the Student's t test. A p value < 0.05 was as significant.

2.2. Bioimpedance measurement

The BIA instrument (QuadScan 4000; Bodystat, Ltd., Isle of Man, UK), which has independent detecting electrodes and current source electrodes in platform and handle grips, was modified by us to enable switching from various arm sides to various leg sides. After calibrating by resistance instrument with high resolution, we confirmed that no other errors occurred in this modification. As shown in Fig. 1, the participants easily stood at the platform embedded with tetra−polar electrodes (E3, E4, E7 and E8) and griped a handle embedded with bipolar electrodes (E1, E2, E5 and E6) in the right−hand side to measure the BIA values by frequency at 50 kHz and current at 400 μA. The E1, E3, E5 and E7 were defined as measuring electrodes and E2, E4, E6 and E8 as current electrodes. All electrodes were made of stainless steel with highly electric conduction to form a current loop at 50 kHz and 400 μA. The bioelectrical impedance value for the whole body was termed Z_{Whole}, right arm segment as Z_{RA}, trunk segment as Z_{RT}, left leg segment as Z_{LL} and right leg segment as Z_{RL}[11]. The different loops were formed by automatically switching program. For example, at the loop between E2 and E4, we can obtain Z_{Whole} values measured between E1 and E3 and Z_{RL} values between E3 and E7. At the loop between E6 and E8, we can obtain Z_{LL} values measured between E3 and E7.

2.3. Experimental procedures

Bodyweight was evaluated by a scale that is accurate to 0.1 kg and body height by a ruler that is accurate to 0.5 cm when

Table 2
Body compositions as measurements by DXA.

Region and item	Male (n = 22)		Female (n = 16)	
	Mean (SD)	Range	Mean (SD)	Range
FFM_{LL-DxA} (kg)	8.34 (0.79)	7.38−10.40	5.82 (0.71)	4.71−7.40
FFM_{RL-DxA} (kg)	8.49 (0.87)	7.18−10.62	5.87 (0.65)	4.75−7.19
$Tissue_{LL-DxA}$ (kg)	10.77 (1.21)	9.04−13.33	9.49 (0.99)	7.79−11.61
$Tissue_{RL-DxA}$ (kg)	10.96 (1.33)	9.07−13.67	9.59 (1.02)	7.96−11.73
FM_{LL-DxA} (%)	22.22 (5.13)	12.50−30.20	38.57 (5.50)	29.30−50.30
FM_{RL-DxA} (%)	22.21 (5.13)	12.40−30.20	38.51 (5.57)	29.30−50.32

All the values were measured by DXA. FFM_{RL-DxA}, FFM in the right-side leg; FFM_{LL-DxA}, FFM in the left-side leg; $Tissue_{RL-DxA}$, the tissue weight in right-side leg; $Tissue_{LL-DxA}$, the tissue weight in both legs. FM_{RL-DxA},FM in the right-side leg; FM_{LL-DxA}, FM in the left-side leg.

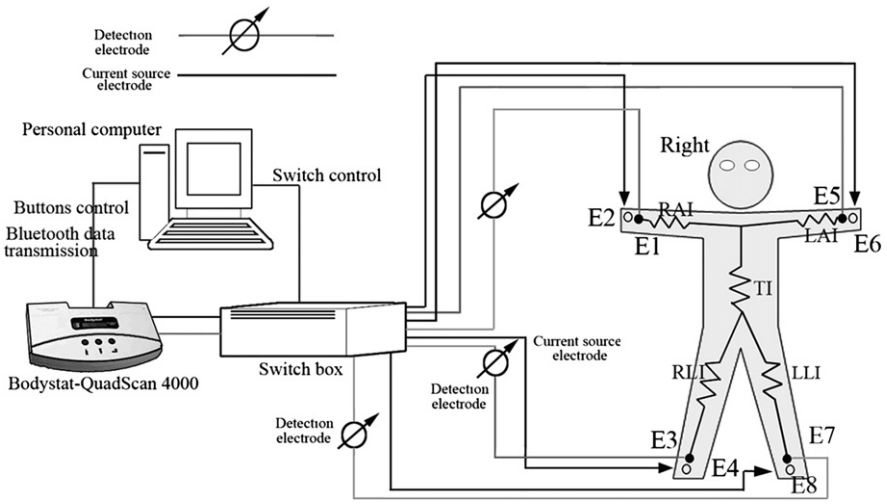

Fig. 1. Measuring platform and bioelectric impedance measurement of the improved system. E1, E3, E5, and E7, current electrode; E2, E4, E6, and E8, measuring electrode; LAI, left arm impedance; LLI, left leg impedance; RAI, right arm impedance; RLI, right leg impedance; TI, trunk impedance.

participants are standing vertically. All of participants, who wore cotton gowns without any metal attachments, were scanned by whole−body DXA (Lunar Prodigy, GE Corp, USA.) at 20 μGy for 20 min. Data from different segments were analyzed by the software enCore 2003 version 7.0 to obtain the FFM in the right−side leg as FFM_{RL-DxA}, in the left−side leg as FFM_{LL-DxA}, and in both legs as $FFM_{leg-DxA}$; the tissue weight in the right−side leg as $Tissue_{RL-DxA}$, in the left−side leg as $Tissue_{LL-DxA}$, and in both legs as $Tissue_{leg-DxA}$. The measurements were all performed by well trained medical technologists with registered licenses in the Department of Radiology, Dah Li County Jen−Ai Hospital, Taiwan. Bone mineral density, total body fat and fat−free mass were estimated. All of the BIA data in each segment are in Table 3.

2.4. Statistical analysis

Data were analyzed by SPSS.14.0 software (SPSS Inc., Chicago, IL, USA). Data are shown as mean ± SD. A confidence level of 5 % ($p < 0.05$) was set as significant. To assay the correlation of estimated FFM values by the linear regression model or by the BIA with BP−ANN model with DXA measurement, r^2 correlation values from Pearson analysis were calculated. The predictive FFM values in both legs by the BIA with linear regression model ($FFM_{leg-linear}$) or by the BIA with BP−ANN model ($FFM_{leg-ANN}$) were compared to DXA measurement ($FFM_{leg-DxA}$). Also, the predictive FFM values from the right−side leg by BIA with linear regression model ($FFM_{RL-linear}$), from the left−side ($FFM_{LL-linear}$) or right−side leg by BIA with BP−ANN model (FFM_{RL-ANN}), and from the left−side leg (FFM_{LL-ANN}) were compared with the DXA measurements. We defined $Tissue_{leg-ANN} = Tissue_{RL-ANN}$ or $Tissue_{LL-ANN}$ and $FFM_{leg-ANN} = FFM_{RL-ANN}$ or FFM_{LL-ANN}.

Table 3
Bioelectrical impedance values measurements by BIA.

Region and item	Male (n = 22)		Female (n = 16)	
	Mean (SD)	Range	Mean (SD)	Range
Z_{LL} (ohm)	230.2 (20.4)	193−264	243.6 (33.2)	182−301
Z_{RL} (ohm)	227.8 (18.9)	187−258	248.6 (30.3)	192−308
Z_{Whole} (ohm)	555.4 (40.2)	447−622	626.9 (58.7)	465−724

The Z_{LL} (bioelectrical impedance values) were measured by current from E6 through E8 and measuring from E3 through E7, The Z_{RL} (bioelectrical impedance values) were measured by current from E2 through E4 and measuring from E3 through E7, Z_{whole} (bioelectrical impedances values) in whole body.

We constructed the FFM estimating system by BIA measurement with the BP−ANN mathematic model (Fig. 2), which is composed of an input layer, hidden layer and output layer[39]. The input layer input five p_j (j = 1−6) values, including age (y), height (h), weight (m), sex (S), Z_{whole}, Z_{RL}, and Z_{LL}. The hidden layer contained one to multiple neuron units as the combination of both of $W^1_{i,j}$ (weight matrix) and b^1_i (bias vector). In other words, both $\mathbf{W}^1_{i,j}$ (weight matrix) and $\mathbf{b}^1_i$ (bias vector) were input to calculate and obtain the $\mathbf{n}^1_i$ value, which was subsequently input into f^1 (transfer function), by the Log−Sigmoid function, to give the $\mathbf{a}^1_i$. $\mathbf{a}^1_i$ acted as the first hidden layer. The above can also be expressed as the following equation:

$$\mathbf{a}^1_i = \mathbf{f}^1\left(\mathbf{W}^1_{i,j}\mathbf{p}_j + \mathbf{b}^1_i\right) = \mathbf{f}^1(\mathbf{n}^1_i) = \text{logsig}\left(\mathbf{W}^1_{i,j}\mathbf{p}_j + \mathbf{b}^1_i\right) \quad (1)$$

$$\text{logsig}(n) = \frac{1}{1+e^{-n}}$$

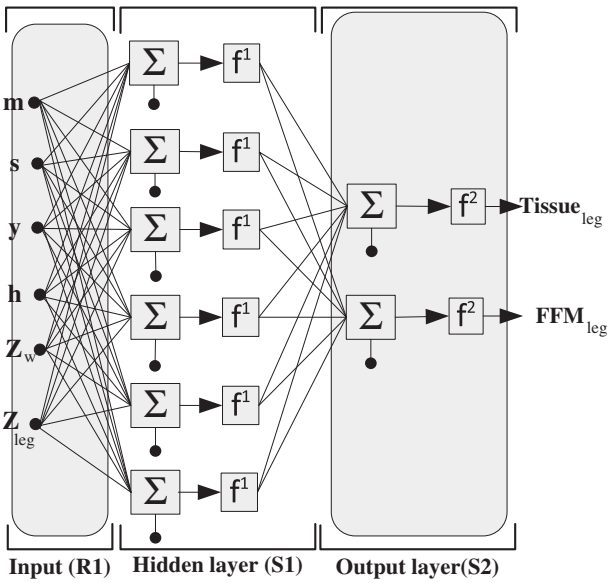

Fig. 2. The BP-ANN in the present study. The input layer (R1) contained six parameters as weight (m), sex (s), age (y), height (h), bioelectrical impedances values in lower limbs (Z_{leg}) and bioelectrical impedances values in whole body (Z_{whole}). The hidden layer (S1) contained six neuron units, f^1 transfer functions for hidden layer and f^2 transfer functions for output layer. The output layer contained two neuron units to outcome the amount of tissue weight of lower limbs ($Tissue_{leg}$) and the amount of the FFM of leg (FFM_{leg}).Σ, was the summation function.

Table 4
the predictive body compositions by linear regression model and by BP−ANN model.

Method	Region and item	Male (n = 22)		Female (n = 16)	
		Mean (SD)	Range	Mean (SD)	Range
Linear Regression	$Tissue_{RL-linear}$ (kg)	10.87 (0.85)	9.45−12.50	9.54 (1.09)	6.77−11.72
	$Tissue_{LL-linear}$ (kg)	10.86 (0.85)	9.41−12.50	9.55 (1.04)	6.91−11.36
	$FFM_{RL-linear}$ (kg)	8.42 (0.54)	7.64−9.53	5.85 (0.69)	4.06−6.77
	$FFM_{LL-linear}$ (kg)	8.42 (0.54)	7.62−9.49	5.85 (0.68)	4.13−6.84
	$FM_{RL-linear}$ (%)	22.34 (4.14)	16.29−31.86	38.62 (2.91)	32.15−43.73
	$FM_{LL-linear}$ (%)	22.32 (4.17)	15.71−31.67	38.67 (2.76)	38.87−43.51
BP−ANN	$Tissue_{RL-ANN}$ (kg)	10.90 (1.19)	9.01−13.44	9.55 (1.07)	7.59−11.90
	$Tissue_{L-ANN}$ (kg)	10.83 (1.15)	9.01−13.44	9.53 (0.96)	7.93−11.73
	FFM_{RL-ANN} (kg)	8.41 (0.74)	7.53−10.29	5.90 (0.67)	4.66−7.03
	FFM_{LL-ANN} (kg)	8.42 (0.74)	7.55−10.31	5.81 (0.65)	4.82−7.07
	FM_{RL-ANN} (%)	22.54 (4.81)	13.14−30.76	38.03 (5.11)	29.28−49.08
	FM_{LL-ANN} (%)	21.94 (4.94)	11.56−30.70	38.99 (4.31)	31.21−46.86

The predictive FFM values in both legs by BIA with the linear regression model. $FFM_{RL-linear}$, FFM in the right-side leg; $FFM_{LL-linear}$, FFM in the left-side leg; $FM_{RL-linear}$, FM in the right-side leg; $FM_{LL-linear}$, FM in the left-side leg; $Tissue_{RL-linear}$, the tissue weight in the right-side leg; $Tissue_{LL-linear}$, the tissue weight the in left-side leg. The predictive FFM values in both legs by BIA with the Back Propagation Artificial Neural Network (BP-ANN) mathematical model. FFM_{RL-ANN}, FFM in the right side leg; FFM_{LL-ANN}, FFM in the left-side leg; FM_{RL-ANN}, FM the in right-side leg; FM_{LL-ANN}, FM in the left-side leg; $Tissue_{RL-ANN}$, the tissue weight in the right-side leg; $Tissue_{LL-ANN}$, the tissue weight the in left-side leg.

Scalars − small *italic* letters
Vectors − small **bold** nonitalic letters
Matrices − capital **BOLD** nonitalic letters
i−the series number of neuron
j−the numbers of input values ($\mathbf{p}_1$ = m, $\mathbf{p}_2$ = s, $\mathbf{p}_3$ = y, $\mathbf{p}_4$ = h, $\mathbf{p}_5 = Z_{whole}$, $\mathbf{p}_6 = Z_{RL}$ or Z_{LL})

The obtained values as $\mathbf{a}^1$ were connected to $\mathbf{f}^2$ (Linear transfer function), which act as the output layer. We expressed the above as the following equation:

$$\mathbf{a}^2 = \mathbf{f}^2(\mathbf{W}^2_{i,1}\mathbf{a}^1_i + \mathbf{b}^2_1) = \mathbf{f}^2(\mathbf{n}^2_1) = \text{purelin}(\mathbf{W}^2_{i,1}\mathbf{a}^1_i + \mathbf{b}^2_1) \quad (2)$$

purelin (n) = a

The output layer with a single hidden layer in our BP−ANN mathematical model was expressed as the following equation:

$$\begin{aligned}\mathbf{a}^2_1 &= \mathbf{f}^2\left(\mathbf{W}^2_{i,1}\mathbf{f}^1\left(\mathbf{W}^1_{i,j}\mathbf{p}_j + \mathbf{b}^1_i\right) + \mathbf{b}^2_1\right) \\ &= \text{purelin}\left(\mathbf{W}^2_{i,1}\text{logsig}\left(\mathbf{W}^1_{i,j}\mathbf{p}_j + \mathbf{b}^1_i\right) + \mathbf{b}^2_1\right) \\ &\left(i = 1 \text{ to } 5,\ j = 1 \text{ to } 6\right) \end{aligned} \quad (3)$$

All of the anthropometric values of height, weight, age, sex and bioelectrical impedances acted as $\mathbf{p}_j$ values in the input layer. They were weighted for every one equation in the initial weight matrix as $\mathbf{W}^1{}_{i,j}$, $\mathbf{W}^2{}_{i,1}$, randomly in the first training procedure, and subsequently were added to initial values in bias vectors as $\mathbf{b}^1{}_i$, $\mathbf{b}^2{}_1$ to obtain the net input values. $f^1$and f^2, types of Log−Sigmoid function, act as transfer functions in the hidden layer and output layer, respectively. These two neurons in the output layer can calculate the weight of the lower limbs ($Tissue_{leg-ANN}$) and the FFM of the legs ($FFM_{leg-ANN}$). As the training rule in the present work, we set the maximum iteration as 1000 times with a minimum gradient value of 10^{-6}. All of the BP−ANN algorithms were coded by Matlab Ver.7.0 (MathWorks, Inc. MA, USA). In our work, we adopted the 2−C model to obtain the percentage of FM (FM%) by the amount of total body weight and FFM in the lower limbs. The predictive equations of tissue FM in the lower limbs (FM_{leg}) were described by the following equations (4):

$$FM_{leg-DXA}\% = \left(Tissue_{leg-DXA} - FFM_{leg-DXA}\right) \Big/ Tissue_{leg-DXA} \times 100\% \quad (4a)$$

$$FM_{leg-ANN}\% = \left(Tissue_{leg-ANN} - FFM_{leg-ANN}\right) \Big/ Tissue_{leg-ANN} \times 100\% \quad (4b)$$

$$FM_{leg-linear}\% = \left(Tissue_{leg-linear} - FFM_{leg-linear}\right) \Big/ Tissue_{leg-linear} \times 100\% \quad (4c)$$

3. Results

From the independent variables of height, weight, age, sex and bioelectrical impedances (Table 1 and Table 3) and the dependent variables of FFM values measured by DXA (Table 2), we obtained linear equations, including the relationships between $FFM_{leg-linear}$ or tissue weights and $FFM_{leg-DxA}$ by following equations (5) and (6), by statistic regression analysis (Table 4). The r^2, SD and root−mean−square deviation (RMSE) were used as the as correlation coefficient, standard deviation and root mean squared error, respectively. The predictive FFM of legs ($FFM_{leg-linear}$) was obtained by following linear regression equation (5):

$$\begin{aligned} FFM_{leg-linear}(kg) &= -4.497 - 0.023\,y + 0.090\,h + 0.013\,m \\ &\quad +1.083\,s - 0.009\,Z_{leg} - 0.001\,Z_{whole} \\ &\left(\text{We defined } FFM_{leg-linear} = FFM_{RL-linear} \text{ or } FFM_{LL-linear} \right. \\ &\quad \left. \text{and } Z_{leg} = Z_{RL} \text{ or } Z_{LL}\right) \\ &\left(R^2 = 0.895,\ SD = 0.502\ kg,\ RMSE = 0.229\ kg\right) \end{aligned} \quad (5)$$

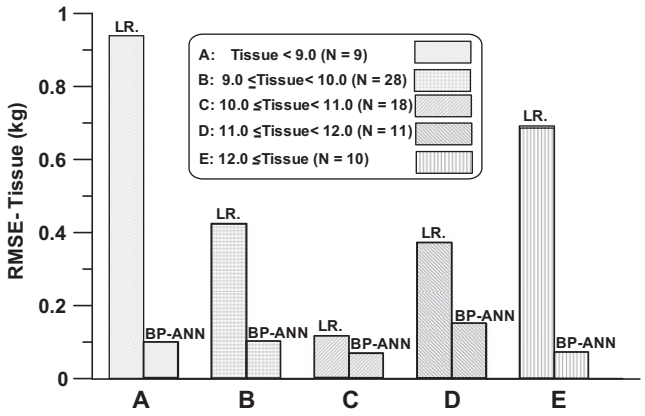

Fig. 3. The RMSE values of predictive tissue (kg) from linear regression equation and BP-ANN corresponding to five subgroups in subjects. All of the subjects were divided into five subgroups based on different ranges of tissues weight. A, Tissue≤ 9.0; B, 9.0 ≤ Tissue < 10.0; C, 10.0 ≤ Tissue < 11.0 ; D, 11.0 ≤ Tissue < 12.0 ;E, 12.0 < Tissue.

Table 5
Correlations between body compositions measurements by DXA and bioelectrical impedance values measurements by BIA.

	Z_{Whole}	Z_{RL}	Z_{LL}	$FFM_{Whole\text{-}DXA}$	$FFM_{RL\text{-}DXA}$	$FFM_{LL\text{-}DXA}$	$Tissue_{RL\text{-}DXA}$	$Tissue_{LL\text{-}DXA}$
Z_{Whole}	1.00							
Z_{RL}	0.84							
Z_{LL}	0.87	0.95	1.00					
$FFM_{Whole\text{-}DXA}$	-0.69	-0.53	-0.51	1.00				
$FFM_{RL\text{-}DXA}$	-0.58	-0.44	-0.40	0.94	1.00			
$FFM_{LL\text{-}DXA}$	-0.57	-0.43	-0.41	0.94	0.99	1.00		
$Tissue_{RL\text{-}DXA}$	-0.47	-0.52	-0.46	0.69	0.77	0.74	1.00	
$Tissue_{LL\text{-}DXA}$	-0.44	-0.51	-0.48	0.69	0.75	0.76	0.97	1.00

The Z_{LL} (bioelectrical impedance values) were measured by current from E6 through E8 and measuring from E3 through E7, The Z_{RL} (bioelectrical impedance values) were measured by current from E2 through E4 and measuring from E3 through E7, Z_{whole} (bioelectrical impedances values) in whole body. All the values were measured by DXA. $FFM_{Whole\text{–}DXA}$, FFM in whole body; $FFM_{RL\text{–}DXA}$, FFM in the right-side leg; $FFM_{LL\text{–}DXA}$, FFM in the left-side leg; $Tissue_{RL\text{–}DXA}$, the tissue weight in the right-side leg; $Tissue_{LL\text{–}DXA}$, the tissue weight in both legs.

The predictive $Tissue_{leg-linear}$ was obtained by following linear regression equation (6):

$$\begin{aligned} Tissue_{leg-linear}(kg) &= -6.960 + 0.013\,y + 0.071\,h + 0.078\,m \\ &\quad -0.028\,s - 0.020\,Z_{leg} - 0.008\,Z_{whole} \end{aligned}$$

$$\left(\text{We defined } Tissue_{leg-linear} = Tissue_{RL-linear} \text{ or } Tissue_{LL-linear} \text{ and } Z_{leg} = Z_{RL} \text{ or } Z_{LL}.\right)$$

$$\left(R^2 = 0.739,\ SD = 0.705\ kg,\ RMSE = 0.452\ kg\right) \quad (6)$$

h: height (Meter)
m: weight (Kilogram)
y: age (Years)
Z_{whole}, Z_{leg} : bioelectrical impedances values in whole body (Z_{whole}) and in lower limbs (Z_{leg}) (Ohm)
S: sex (1: male, 0: female)
FFM: Free fat mass (kilogram)
Tissue: Tissue weight (kilogram)

In our BP–ANN mathematically predictive model, which contained single hidden layer with six neurons and two output layers, by a training procedure to get the optimal weight values and bias vectors, it was possible to measure $FFM_{leg-ANN}$ and tissue weight in the lower limbs of elderly participants. To observe whether the deviation of errors exist in various distributions, we compared the RMSE of $FFM_{leg-linear}$ *vs* $FFM_{leg-DxA}$ and of $FFM_{leg-ANN}$ *vs* $FFM_{leg-DxA}$ in each of the five distributions by tissue weight at the first (Fig. 3). In other words, given that the relationships between $FFM_{leg-linear}$ and $FFM_{leg-DxA}$ are real linear regression relationships, little or no deviation of errors exist in various distributions. The five distributions were as follows: A: Tissue <9.0 kg (N = 9), B: 9.0 kg ≤ Tissue < 10.0 kg (N = 28), C: 10.0 kg ≤ Tissue < 11.0 kg (N = 18), D: 11.0 kg ≤ Tissue<12.0 kg (N = 11) and E: 12.0 ≤ Tissue (N = 10).

The RMSE of $FFM_{leg-linear}$ *vs* $FFM_{leg-DxA}$ and of $FFM_{leg-ANN}$ *vs* $FFM_{leg-DxA}$ in each separated five distributions by tissue weight were 0.930 kg, 0.423 kg, 0.117 kg, 0.327 kg and 0.686 kg in the linear regression predictive models, and 0.100 kg, 0.103 kg, 0.069 kg, 0.162 kg and 0.073 kg in the BP–ANN predictive models, respectively. The RMSE of $FFM_{leg-ANN}$ *vs.* $FFM_{leg-DxA}$ exhibited much lower levels. At the second, to show that deviation of errors exist in predictive tissue weights of FFM, we compared the Bland –Altman Plot of predictive tissue weights of $FFM_{leg-ANN}$ *vs.* $FFM_{leg-DxA}$ (Fig. 4A) with that of $FFM_{leg-linear}$ *vs.* $FFM_{leg-DxA}$ (Fig. 4B). The greater distributing range of deviations in $FFM_{leg-linear}$ *vs* $FFM_{leg-DxA}$ than in $FFM_{leg-ANN}$ *vs* $FFM_{leg-DxA}$ (2 SD=0.56 kg than 2 SD = 0.96 kg) were obtained. The deviation of errors in predictive tissue weights in the lower limbs by linear regression compared with by BP–ANN were also observed in the same way as mentioned above (Fig. 5) (2 SD = 0.63 kg than 2 SD = 1.35 kg). The deviation of errors in predictive tissue fat in the lower limbs by linear regression compared with by BP–ANN were also observed in the same way as mentioned above (Fig. 6) (mean = 0.01%, 2 SD = 3.64% than mean = 0.12%, 2 SD = 7.68%). The lower deviation of errors in predictive tissue fat and in the lower limbs of $FFM_{leg-ANN}$ *vs* $FFM_{leg-DxA}$ exhibited much lower levels. To compare the correlation of $FFM_{leg-ANN}$ *vs* $FFM_{leg-DxA}$ and that of $FFM_{leg-linear}$ *vs* $FFM_{leg-DxA}$, the relationships of the predictive Tissue value by the linear regression model and by the BP–ANN model *vs* the measured Tissue values by DXA are shown in Fig. 7. Relative correlation existed greater by the BP–ANN model (R^2 = 0.962) than by the linear regression model (r^2 = 0.846). The correlations between BIA values, which include Z_W, Z_{LL} and Z_{RL}, and measured DXA values, which include $FFM_{RL\text{–}DxA}$, $FFM_{LL\text{–}DxA}$ and $FFM_{leg\text{–}DxA}$, are shown in Table 5. The correlations between Z_{whole} and Z_{RL}, Z_{LL}, $FFM_{RL\text{–}DxA}$, $FFM_{LL\text{–}DxA}$, $Tissue_{RL\text{–}DxA}$ and $Tissue_{LL\text{–}DxA}$ were 0.84, 0.87, −0.58, −0.57, −0.47

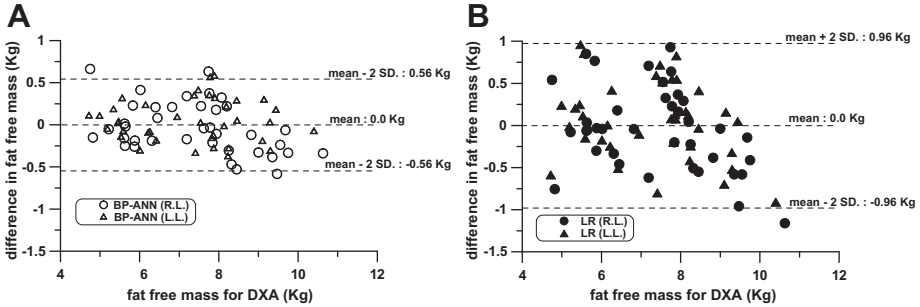

Fig. 4. The distribution of errors in predictive tissue weights of $FFM_{leg-ANN}$ *vs* $FFM_{leg-DxA}$ (Fig. 4A) and that of $FFM_{leg-linear}$ *vs*. $FFM_{leg-DxA}$ (Fig. 4A). The predictive tissue weights of $FFM_{leg-ANN}$ in right side (also as FFM_{RL-ANN}) were symbolized as ○ and in left (also as FFM_{LL-ANN})as △ and that of $FFM_{leg-linear}$ in right side (also as $FFM_{RL-linear}$) as ● and in left (also as $FFM_{LL-linear}$) as ▲.

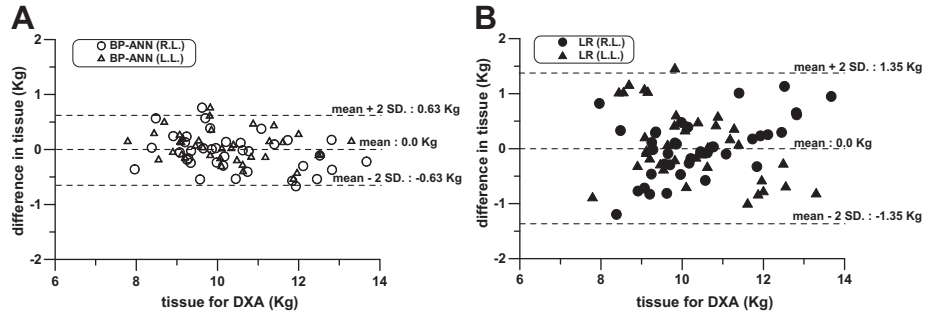

Fig. 5. The distribution of errors in predictive tissue weight of lower limbs ($Tissue_{leg-ANN}$) *vs* $Tissue_{leg-DxA}$ (Fig. 5A) and that of $Tissue_{leg-linear}$ *vs* $Tissue_{leg-DxA}$ (Fig. 5B). The predictive tissue weights of $Tissue_{leg-ANN}$ in right side (also as $Tissue_{RL-ANN}$) were symbolized as ○ and in left side (also as $Tissue_{LL-ANN}$) as △ and that of $Tissue_{leg-linear}$ in right side (also as $Tissue_{RL-linear}$) as ● and in left (also as $Tissue_{LL-linear}$) as ▲.

and −0.44, respectively. There were low correlations between Z_{whole}, Z_{RL}, Z_{LL}, $Tissue_{RL-DxA}$ and $Tissue_{LL-DxA}$ and each other, except for Z_{RL} *vs* Z_{LL}, $Tissue_{RL-DxA}$ *vs* $Tissue_{LL-DxA}$ and FFM_{RL-DxA} *vs* FFM_{LL-DxA}.

4. Discussion

The novel BP−ANN mathematically predictive model of BIA measurement of body composition in the lower limbs of elderly participants in a standing position was successfully developed and performed well, especially when compared with that of the traditional linear regression. We tried to compare the *r* value, r^2 value, 2 SD and RMSE to elucidate whether both the precision and accuracy of the BP−ANN mathematically predictive model in BIA measurement of body compositions in the lower limbs of elderly participants are greater than that of traditional linear regression. Compared with the differences of $FFM_{leg-ANN}$ *vs* $FFM_{leg-DxA}$ to $FFM_{leg-linear}$ *vs* $FFM_{leg-DxA}$, the lower 2 SD in $FFM_{leg-ANN}$ *vs* $FFM_{leg-DxA}$ shows that the BP−ANN mathematically predictive model exhibited greater precision and accuracy in prediction of FFM. Notably, these data were much lower than that reported by from Jaffrin[18] and Bracco[14,15]. Similarly, we compared the differences in tissue weight in the lower limbs from ANN *vs* DXA and from linear *vs* DXA; the lower 2 SD in ANN *vs* DXA also indicated greater performance of the BP−ANN mathematically predictive model. In other words, the much wilder distributing range of deviations in each predictive FFM value by linear *vs* DXA than by ANN *vs* DXA also shows that the FFM predictive model is not suitable to the linear regression model; accordingly, the issues about development of non−linear predictive models and/or other more flexibly changeable mathematic ones to describe the relationships among the body compositions (fat free mass) and other multiple parameters require much more attention to improve predictive accuracy. From the obtained tissue weights in lower limbs ($Tissue_{leg}$) and FFM_{leg} by ANN or by the linear equation, we could calculate the tissue fat in lower limbs ($TFM_{leg-ANN}$ %) or ($TFM_{leg-linear}$ %). Also, greater performance of the BP−ANN mathematically predictive model was observed. With such multiple dependent and/or independent variables, including height, age, weight, sex and bioelectrical impedances, in the development of the predictive model, we assumed that the system should be complex rather than a simple linear regression model. The lower correlations between Z_{whole}, Z_{LL}, FFM_{LL-DxA} and $Tissue_{LL-DxA}$ and each other indicated that it is not feasible to adopt the linear equation for prediction of body composition. By the use of totally different weight coefficients in every variable in our predictive equations such as equations (5) and (6), again, we can also assume that it is not linear regression. The relationships between body composition and weight, height and age as a non−linear model has been reported[40]. In fact, the ANN, because the multiple programs compute by mimicking multiple inputs with non−linear interactions between each other at high speed, was essentially created to calculate the complex model[41]. As mentioned above, the lower correlations between Z_{whole}, Z_{LL}, FFM_{LL} and $Tissue_{LL}$ and each other shows the greater performance in prediction by ANN in our study. Besides, the most optimal weight matrix and bias vector were acquired after a serial learning procedure. Given that the predictive model fits with the linear regression model, the five separated distributions by tissue weight should exhibit similarly lower RMSE in each distribution. In fact, there were totally different RMSE in each distribution when we analyzed by the linear model. In contrast, the much lower RMSE with a similar amount in each distribution existed when we analyzed by the ANN model. Notably, the RMSE in five distributions were almost the same by the ANN model. The RMSE provides an index of the extent of predictive accuracy; consequently, the ANN model was a successful model. To prevent from the occurrence of over−fitting at hyper hidden layers and neurons with

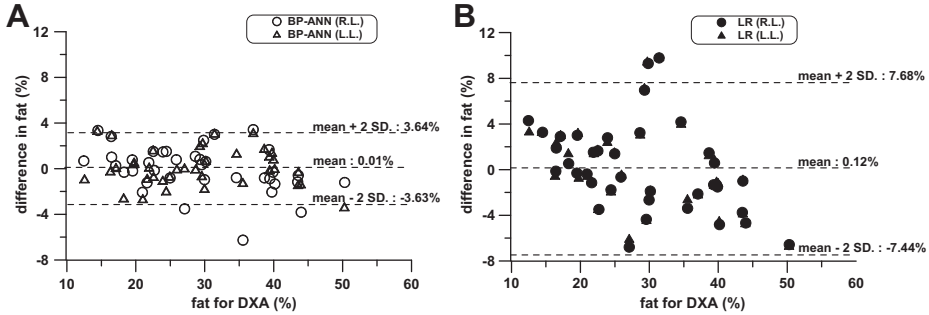

Fig. 6. The distribution of errors in predictive tissue fat mass of lower limbs ($FM_{leg-ANN}$) *vs* $FM_{leg-DxA}$ (Fig. 6A) and that of $FM_{leg-linear}$ *vs*. $FM_{leg-DxA}$ (Fig. 6B). The predictive tissue weights of $FM_{leg-ANN}$ in right side (also as FM_{RL-ANN}) were symbolized as ○ and in left (also as FM_{LL-ANN}) as △ and that of $FM_{leg-linear}$ in right side (also as $FM_{RL-linear}$) as ● and in left (also as $FM_{LL-linear}$)as ▲.

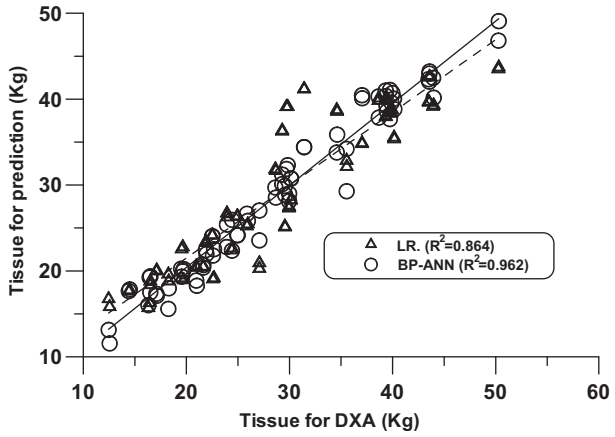

Fig. 7. The relationship of the predictive Tissue value by linear regression equation (Tissue $_{leg-linear}$) and BP-ANN mode (Tissue$_{leg-ANN}$) *vs*. the measured Tissue values by DXAo.

hypo inputs, we employed single hidden layer and six neurons as well as Bayesian regularization to operate training procedures[42]. There are many papers about the application of BIA in the prediction of lean tissue mass[21], FFM[18,19] and total body water[43], however are predicted by the mathematical linear model. Collectively, we tried to compare the variations of predictive FFM of the lower limbs of elderly participants by BIA measurement with the BP–ANN mathematical models and with linear regression models. The results have shown the superior outcomes with the BP–ANN model and have pointed out the successful applicability in prediction of FFM of the lower limbs of elderly participants.

References

1. Janssen I, Heymsfield SB, Ross R. Low relative skeletal muscle mass (sarcopenia) in older persons is associated with functional impairment and physical disability. *J Am Geriatr Soc*. 2002;50:889–896.
2. Baumgartner RN, Koehler KM, Gallagher D, et al. Epidemiology of sarcopenia among the elderly in New Mexico. *Am J Epidemiol*. 1998;147:755–763.
3. Melton LJ 3rd, Khosla S, Crowson CS, et al. Epidemiology of sarcopenia. *J Am Geriatr Soc*. 2000;48:625–630.
4. Borkan GA, Hults DE, Gerzof SG, et al. Age change in body composition revealed by computed tomography. *J Gerontol*. 1983;38:673–677.
5. Movak LP. Aging, total body potassium, fat–free mass, and cell mass in males and females between ages 18 and 85 years. *J Gerontol*. 1972;27:438–443.
6. Noppa H, Andersson M, Bengtsson C, et al. Body composition in middle–aged women with special reference to the correlation between body fat mass and anthropometric data. *Am J Clin Nutr*. 1979;32:1388–1395.
7. Durnin JV, Womersley J. Body fat assessed from total body density and its estimation from skinfold thickness: measurements on 481 men and women aged from 16 to 72 years. *Br J Nutr*. 1997;32:77–97.
8. Lynch NA, Metter EJ, Lindle RS, et al. Muscle quality. I. Age–associated difference between arm and leg muscle groups. *J Appl Physiol*. 1999;86:188–194.
9. Sayer AA, Syddal HE, Martin HJ. Falls, sarcopenia, and growth in early life: findings from the Hertfordshire cohort study. *Am J Epidemiol*. 2006;164:665–671.
10. Baumgartner RN, Waters DL. Predictors of skeletal muscle mass in elderly men and women. *Mech Ageing Dev*. 1999;107:123–136.
11. Ellis KJ. Human body composition: in vivo methods. *Physiol Rev*. 2001;80: 649–680.
12. Bussolotto M, Ceccon A, Sergi G, et al. Assessment of body composition in elderly: accuracy of bioelectrical impedance analysis. *Gerontology*. 1999:39–43.
13. Kyle UG, Bosaeus I, Lorenzo AD, et al. Bioelectrical impedance analysis—part II: utilization in clinical practice. *Clinical nutrition*. 2004;23:1430–1453.
14. Organ LW, Bradham GB, Gore DT, et al. Segmental bioelectrical impedance analysis: theory and application of a new technique. *J Appl Physiol*. 1994;77: 98–112.
15. Bracco D, Thiebaud D, Chiolero RL, et al. Segmental body composition assessed by bioelectrical impedance analysis and DEXA in humans. *J Appl Physiol*. 1996;81:2580–2587.
16. Stewart SP, Bramley PN, Heighton R, et al. Esitmation of body composition from bioelectrical impedance of body segments: comparison with dual–energy X–ray absorptiometry. *Br J Nutr*. 1993;69:645–655.
17. Zhu F, Schneditz D, Wang E. Dynamic of segmental extracellular volumes during changes in body position by bioimpedance analysis. *J Appl Physiol*. 1998;85:497–504.
18. Jaffrin MY, Morel H. Measurements of body composition in limbs and trunk using a eight contact electrodes impedancementer. *Med Eng Phys*. 2009;31: 1079–1086.
19. Bedogni G, Marra M, Bianchi L. Comparison of bioelectrical impedance analysis and dual–energy X–ray absorptiometry for the assessment of appendicular body compostion in anorexic women. *Eur J Clin Nutr*. 2003;57:1068–1072.
20. Sartorio A, Malavolti M, Agosti F, et al. Body water distribution in severe obesity and its assessment from eight–polar bioelectrical impedance analysis. *Eur Clin Nutr*. 2005;59:155–160.
21. Malavolti M, Mussi C, Poli M, et al. Cross–calibration of eight–polar bioelectrical impedance analysis versus dual–energy X–ray absorptiometry for the assessment of total and appendicular body composition in healthy subjects aged 21–82 year. *Ann Human Biol*. 2003;30:380–391.
22. Colado JC, Triplett NT, Tella V, et al. Effect of aquatic resistance training on health and fitness in postmenopausal women. *Eur J Appl Physiol*. 2009;106:113–122.
23. Neovius M, Hemmingsson E, Freyschuss B, et al. Bioelectrical impedance underestimates total and truncal fatness in abdominally obese women. *Obesity*. 2006;14:1731–1738.
24. Piettoi A, Rubiano F, St–Onge MP, et al. New bioimpedance analysis system: improved phenotyping with whole–body analysis. *Eur J Clin Nutr*. 2004;58: 1479–1484.
25. Guo SS, Chumlea WC, Cockram DB. Use of statistical method to estimate body composition. *Am J Clin Nutr*. 1996;64(Suppl):428S–435S.
26. Watson JH, Sox HC, Neff RK, et al. Clinical prediction rules: applications and methodological standards. *N Engl J Med*. 1985;313:793–799.
27. Bax WG. Application of artificial neural network to clinical medicine. *Lancet*. 1995;346:1135–1138.
28. Penedo MG, Carreira MJ, Mosquera A, et al. Computer–aided diagnosis: a neural–network–based approach to lung nodule detection. *IEEE Trans Med Imag*. 1998;17:872–880.
29. Devine B, Macfarlane PW. Detection of electrocardiographic 'left ventricular strain' using neural nets. *Med Biol Eng Comput*. 1993;31:343–348.
30. Dybowskir R, Vanya G. Artifical neural network in pathology and medical laboratories. *Lancet*. 1995;346:1203–1207.
31. Pedersen PV, Modi NB. Application of neural networks to pharmacodynamics. *J Pharm Sci*. 1993;82:918–926.
32. DiRusso SM, Suillivan Holly C, et al. An artificial neural network as a model for prediction of survival in trauma patients: validation for a regional trauma area. *J Trauma*. 2000;49:212–223.
33. Izenberg SD, Williams MD, Luterman A. Prediction of trauma mortality using a neural network. *Am Surg*. 1997;63:275–281.
34. McCullagh P, Nelder JA. *Generalized linear models*. 2nd ed. London: Champan and Hall; 1989.
35. Cox DR. Regression models and life tables. *J Roy Statist Soc Ser B*. 1972;34:187–220.
36. Mohamed EI, Maiolo C, Linder R, et al. Predicting the intracellular water compartment using artificial neural network analysis. *Acta Diabetol*. 2003;40: S15–S18.
37. Mazess RB, Barden HS, Bisek JP, et al. Dual–energy x–ray absorptiometry for total–body and regional bone–mineral and soft–tissue composition. *Am J Clin Nutr*. 1990;51:1106–1112.
38. Lorenzo AD, Sorge SP, Iacopino L, et al. Fat–free mass by bioelectrical impedance vs dual–energy X–ray absorptiometry (DXA). *Appl Radial Iost*. 1998;49:739–741.
39. Hagan MT, Demuth HB, Beale M. *Neural Network Design, Thomson Learning, Inc*; 1996.
40. Roubenoff R, Dallal GE, Wilson PW. Predicting body fatness: the body mass index vs estimation bioelectrical impedance. *Am J Public Health*. 1995;85:726–728.
41. Cross SS, Harrison RF, Kennedy RL. Introduction to neural networks. *Lancet*. 1995;346:1075–1079.
42. MacKay DJC. A practical Bayesian framework for backpropagation networks. *Neural Computation*. 1992;4:448–472.
43. Bedogni G, Malavolti M, Severi S. Accuracy of an eight–point tactile–electrode impedance method in the assessment of total body water. *Eur J Clin Nutr*. 2002;56:1143–1148.